



University of HUDDERSFIELD

University of Huddersfield Repository

Kendall, S. R. and Rao, H.V.

Detection of multiple solutions using a mid-cell back substitution technique applied to computational fluid dynamics

Original Citation

Kendall, S. R. and Rao, H.V. (2000) Detection of multiple solutions using a mid-cell back substitution technique applied to computational fluid dynamics. Proceedings of the Institution of Mechanical Engineers Part C Journal of Mechanical Engineering Science, 214 (11). pp. 1401-1407. ISSN 09544062

This version is available at <http://eprints.hud.ac.uk/id/eprint/2470/>

The University Repository is a digital collection of the research output of the University, available on Open Access. Copyright and Moral Rights for the items on this site are retained by the individual author and/or other copyright owners. Users may access full items free of charge; copies of full text items generally can be reproduced, displayed or performed and given to third parties in any format or medium for personal research or study, educational or not-for-profit purposes without prior permission or charge, provided:

- The authors, title and full bibliographic details is credited in any copy;
- A hyperlink and/or URL is included for the original metadata page; and
- The content is not changed in any way.

For more information, including our policy and submission procedure, please contact the Repository Team at: E.mailbox@hud.ac.uk.

<http://eprints.hud.ac.uk/>

Detection of multiple solutions using a mid-cell back substitution technique applied to computational fluid dynamics

S R Kendall* and H V Rao

School of Engineering, The University of Huddersfield, West Yorkshire, UK

Abstract: Computational models for fluid flow based on the Navier–Stokes equations for compressible fluids led to numerical procedures requiring the solution of simultaneous non-linear algebraic equations. These give rise to the possibility of multiple solutions, and hence there is a need to monitor convergence towards a physically meaningful flow field. The number of possible solutions that may arise is examined, and a mid-cell back substitution technique (MCBST) is developed to detect and avoid convergence towards apparently spurious solutions. The MCBST was used successfully for flow modelling in micron-sized flow passages, and was found to be particularly useful in the early stages of computation, optimizing the speed of convergence.

Keywords: mid-cell back substitution, computational fluid dynamics, compressible fluids, flow modelling

NOTATION

E_j	error resulting from the back substitution of the mid-cell (y_{im}) values into the original finite difference flow equations
H	passage depth (m)
L_{th}	passage length (m)
m	maximum grid mesh number in the y direction
n	maximum grid mesh number in the x direction
N_2	nitrogen gas
p	pressure (N/m^2)
u	velocity component in the x direction (m)
v	velocity component in the y direction (m)
w	velocity component in the z direction (m)
x, y, z	coordinates (m)
$\Delta x, \Delta y, \Delta z$	grid size in the x, y and z directions (m)
y_{i0}	solution of the unknown values for u, v and p at the nodal points of the flow mesh
y_{im}	extrapolated values for u, v and p at the mid-cell positions of the flow mesh

1 INTRODUCTION

The non-linear nature of the simultaneous algebraic equations encountered in the numerical solution of the Navier–Stokes equations governing the flow of fluid gives rise to the possibility of multiple solutions [1]. However, only one of these numerical solutions will be a true representation of the actual physical flow field. Hence, it is necessary to monitor the convergence of the solution in order to detect and avoid physically meaningless solutions.

In this paper the number of possible numerical solutions that may arise is examined using an alternative approach, which may also be confirmed with the more general technique known as Bezout's theorem [2]. A mid-cell back substitution technique (MCBST) is developed for monitoring solution convergence.

2 THEORY

2.1 Occurrence of multiple solutions in numerical procedures employing the Navier–Stokes equations

The numerical solution of the Navier–Stokes equations based upon the finite difference equations, along with appropriate boundary conditions, may be assumed to result in algebraic equations up to a third degree: $N_1 =$ number of linear algebraic equations; $N_2 =$ number of quadratic algebraic equations; $N_3 =$ number of cubic

The MS was received on 20 August 1999 and was accepted after revision for publication on 10 December 1999.

**Corresponding author: School of Engineering, The University of Huddersfield, Queensgate, Huddersfield, West Yorkshire HD1 3DH, UK.*

algebraic equations. The procedure may readily be extended to accommodate higher than third-order algebraic equations, when necessary.

The total number of algebraic equations, N , is given by

$$N = (N_1 + N_2 + N_3)$$

The above equations are written in terms of the unknown values of u , v and p at various nodal points for a steady state problem. It is shown in the Appendix that the total possible sets of solutions is given by

$$N_{\text{set}} = 2^{N_2} \times 3^{N_3} \tag{1}$$

It is possible that some of these roots may be imaginary.

2.2 Mid-cell back substitution technique

Let the finite difference equations for the unknown u , v and p values at the nodal points within a two-dimensional flow field be represented by the following N equations:

$$f_j(y_1, y_2, \dots, y_N) = 0 \quad \text{for } j = 1, 2, \dots, N \tag{2}$$

where y_i , $i = 1, 2, \dots, N$ are the unknown values of u , v and p at the nodal points.

If y_{i0} , $i = 1, 2, \dots, N$ is one of the solutions to the N algebraic equations, then

$$f_j(y_{10}, y_{20}, \dots, y_{N0}) = 0 \quad \text{for } j = 1, 2, \dots, N \tag{3}$$

The solution of the unknown values for u , v and p are represented by y_{i0} at various grid nodal points shown in Fig. 1, and these y_{i0} values may be used to extrapolate mid-cell values denoted by the symbol y_{im} for $i = 1, 2, \dots, N$.

Using Taylor's expansion [3]

$$y_{im} \approx y_{i0} + \frac{\partial y_i}{\partial x} \left(\frac{\Delta x}{2} \right) + \frac{\partial y_i}{\partial y} \left(\frac{\Delta y}{2} \right)$$

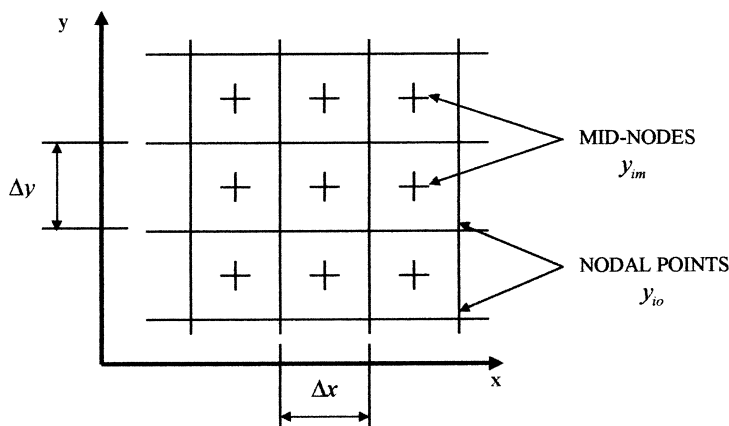


Fig. 1 Two-dimensional flow field depicting the grid system and mid-nodes

Therefore

$$y_{im} = y_{i0} + \delta_i$$

where

$$\delta_i \equiv y_{im} - y_{i0} \tag{4}$$

Substitution of y_{im} , $i = 1, 2, \dots, N$ into the functions f_j , $j = 1, 2, \dots, N$ defined in equation (2) provides magnitudes of f_j that are equated to E_j as defined below:

$$E_j = f_j(y_{1m}, y_{2m}, \dots, y_{Nm}), \quad j = 1, 2, \dots, N \tag{5}$$

where E_j , $j = 1, 2, \dots, N$ represent the 'error' resulting from the back substitution of the mid-node (y_{im}) values into equation (2); E_j may alternatively be expressed as follows:

$$\begin{aligned} E_j &= f_j(y_{1m}, y_{2m}, \dots, y_{Nm}) - f_j(y_{10}, y_{20}, \dots, y_{N0}) \\ &= \sum_{i=1}^{i=N} \left[\left(\frac{\partial f_j}{\partial y_i} \right)_{y_i=y_{i0}} \delta_i \right] \\ &\quad + (\text{terms of } \delta_i \text{ raised to the power of 2 and above}) \end{aligned} \tag{6}$$

where δ_i are defined in equation (4).

The partial derivatives $(\partial f_j / \partial y_i)_{y_i=y_{i0}}$ may have magnitudes that result in the following possible inequalities:

$$\frac{E_{\text{max}}}{\delta_{\text{min}}} < E_0 \tag{7}$$

$$\frac{E_{\text{min}}}{\delta_{\text{max}}} > E_0 \tag{8}$$

where

$\delta_{\text{min}} \equiv$ minimum of the absolute values of δ_i , $i = 1, 2, \dots, N$

$\delta_{\text{max}} \equiv$ maximum of the absolute values of δ_i , $i = 1, 2, \dots, N$

E_{\min} \equiv minimum of the absolute values of E_j , $j = 1, 2, \dots, N$

E_{\max} \equiv maximum of the absolute values of E_j , $j = 1, 2, \dots, N$

E_0 = a positive number suitably selected dependent upon the grid aspect ratio ($\Delta y/\Delta x$), usually having a value between 1 and 10.

If the solution of the y_{i0} values are such that the inequality in (7) is valid, then the solution is considered acceptable. If inequality (8) is true, then the corresponding solution is rejected.

2.3 Principle of the back substitution technique

If the y_{im} values were inserted into the equations represented by (2), they would result in an error E_j , as given in equation (5). Where the condition given by inequality (7) is satisfied, the maximum error E_{\max} will be small. On the other hand, if the solutions for y_{i0} result in E_j values that satisfy the condition given in inequality (8), then this will lead to a large value of E_{\max} .

In the mid-cell back substitution procedure described in Section 2.2, a sequence of iterates is generated that converges to the solution of the system, provided that the initial approximations, y_{i0} , derived from the inlet boundary conditions, are sufficiently close to the true solution. By monitoring the convergence of the solution using the mid-cell substitution extrapolations, any divergence of the generated errors can be detected at an early stage in the solution procedure. The initial approximations y_{i0} may then be adjusted within pre-determined increments and limits, and the whole solution procedure reinitiated. Hence the mid-cell back substitution procedure is a means of avoiding solutions y_{i0} that generate large values of $(\partial f_j/y_i)$ leading to excessively large E_j values.

2.4 Computer Resources

The computer used extensively in the solution of the present numerical flow model was a Fujitsu MCCVPX240/10 supercomputer located at the University of Manchester, Oxford Road, Manchester. Access to this computing system was confined to 12 h slots, once or twice a week, depending on overall demand.

3 RESULTS

3.1 Results obtained using an experimental test rig

Experimental and computational programs were conducted with various passage depths measured in micrometres, two fluids and a variety of inlet flowrates as determined by the positive displacement of a piston. Figure 2 shows a schematic layout of the unique

experimental test rig employed in the validation of the computational results.

3.2 Results from the computational model

From experience, the permissible error in the finite difference equations arising from back substitution can be related to the size of the flow field mesh. A satisfactory back substitution error value is governed by the size of the flow field mesh employed.

A weighted correction technique was employed within the iterative solution procedure. Using the dependent variable u as an example of the dependent variables u , v and p , the weighted correction in u is defined as

Weighted correction (u)

$$= \frac{\text{accumulative change in } u \text{ owing to solution procedure}}{\text{accumulative } u \text{ terms}}$$

or

$$\text{Weighted correction } (u) = \frac{\sum[(u_0 \times u')/(u_0 + u')]}{\sum(u_0)} \quad (9)$$

where u_0 is the initial estimate for the u velocity, u' is the change in u_0 as produced by the iterative solution procedure. If the weighted correction in either u , v or p is greater than the desired permissible levels, then new initial estimates are obtained using the following equation, and the whole iterative solution procedure is resumed:

$$u_0 = u_0 + u' \quad (10)$$

To promote stability of a solution, especially in the early stages of convergence, a relaxation factor can be applied to the dependent variables u , v and p by introducing a relaxation coefficient into equation (10) in the following manner:

$$u_0 = u_0 + \alpha_R \times u' \quad (11)$$

The corrections in the dependent variables were determined using the LU decomposition procedure [4], and the relaxation coefficient α_R was usually set between 0 and 1 (i.e. underrelaxation). The optimum relaxation coefficient can vary, dependent upon the type of fluid, the number of nodal points on the finite difference mesh and the mesh spacing itself. Keeping the relaxation coefficient constant throughout the entire convergence procedure was found to be inefficient. Therefore, a system that monitors convergence was incorporated which gradually adjusts the relaxation coefficient in accordance with the convergence trends exhibited by the dependent variables.

Typical results for fluid flow in micron-sized passages can be exemplified by the relationship between the centre-line velocity u of the fluid and the length of passage through which it flows. Figure 3 shows how this

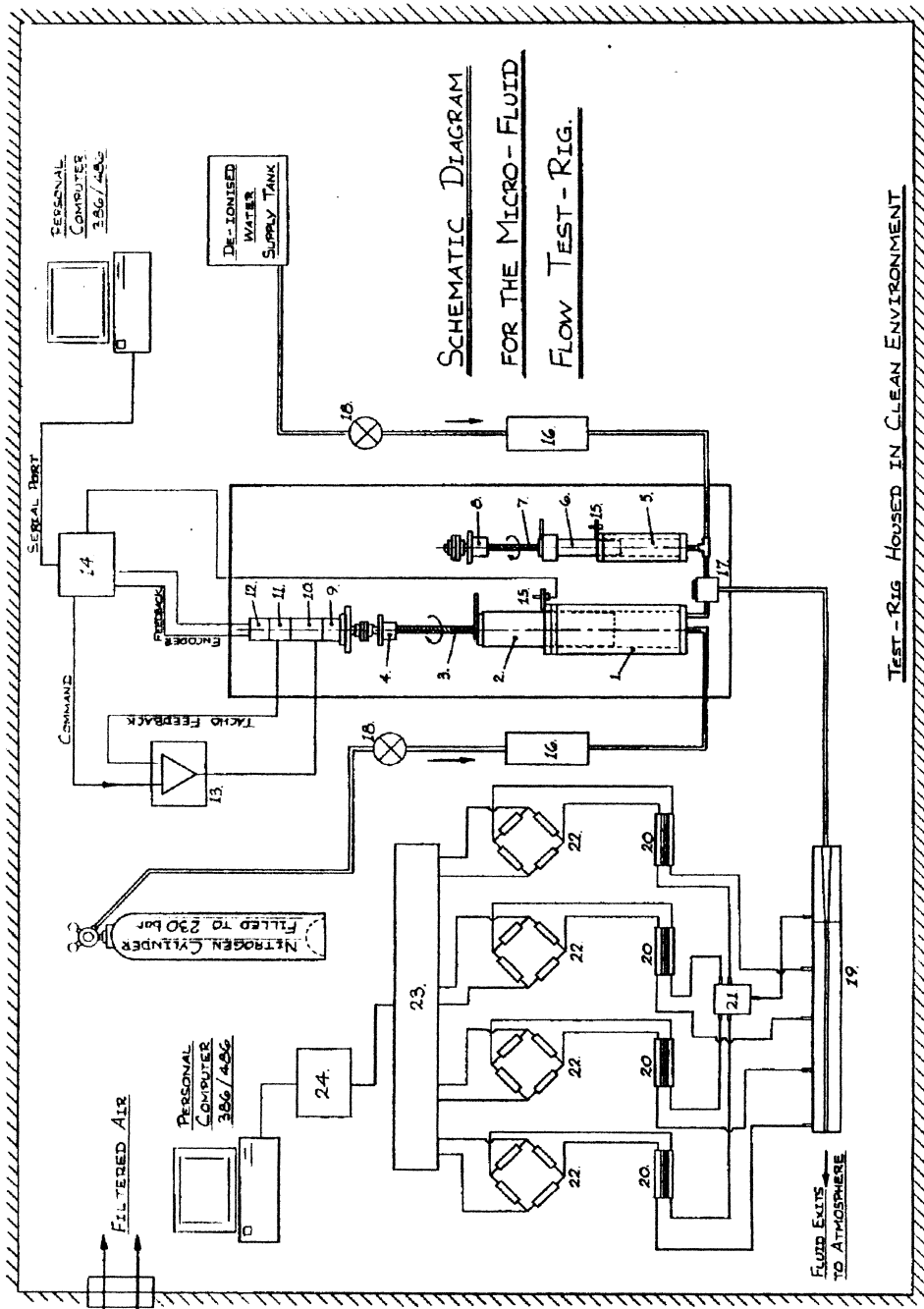


Fig. 2 Schematic drawing of the test rig and ancillary equipment: 1, phosphor bronze cylinder (nitrogen), i.d. = 80 mm; 2, stainless steel piston (nitrogen), o.d. = 80 mm; 3, 16 mm diameter × 2 mm lead precision ball screw; 4, bearing support unit for 16 mm diameter ball screw; 5, phosphor bronze cylinder (water), i.d. = 20 mm; 6, stainless steel piston (water), o.d. = 20 mm; 7, 10 mm diameter × 1 mm lead precision ball screw; 8, bearing support unit for 10 mm diameter ball screw; 9, 43:1 ratio gearhead; 10, d.c. servo motor; 11, tachogenerator; 12, shaft encoder; 13, servo amplifier; 14, motor controller; 15, limit switch; 16, 0.5 µm in-line filter (stainless steel); 17, three-way ball valve (stainless steel); 18, in-line ball valve (stainless steel); 19, micro-sized passage; 20, pressure transducer (diaphragm strain gauge design); 21, micromanifold; 22, strain indicator configured as a full bridge; 23, simultaneous sample and hold board; 24, analogue-to-digital converter

value for the centre-line velocity u initially peaks following inlet to the passageway and then steadies out. It is this type of flow behaviour that benefited from the inclusion of the MCBST because it enhanced the likelihood of the numerical solution converging.

3.3 Comparison of results using the friction factor variable

Since small Reynolds numbers may be associated with micropassage flows, the relationship between the friction factor f and the Reynolds number in laminar steady flows through micron-sized passages was examined. Friction factors were obtained for a range of micropassage flow cases, using both computational and experimentally determined pressure gradients (dp/dx). The Fanning friction factor [5] is defined by the following equation:

$$f = \frac{(dp/dx)D_{eq}}{2\rho_m u_m^2} \quad (12)$$

The friction factors determined from the computational and experimental results are compared with theoretically predicted values for one-dimensional incompressible laminar steady flow [6], given by the following equation:

$$f = \frac{24}{Re} \quad (13)$$

The results for friction factors from the experimental work with micropassages, the corresponding computational results based on two-dimensional laminar steady flow and traditional correlations for one-dimensional fully developed laminar flow between parallel plates are presented in Table 1. The comparison of friction factors determined from computational and experimental

results exhibits a good correlation. The theoretically predicted traditional values are, however, consistently lower than the other two. An error analysis for the experimentally determined friction factors has been carried out.

3.4 Convergence of the computational procedure

The convergence of the numerical solution utilizing a 55 μm deep passageway and nitrogen gas as the working fluid (hence the passage designation N55a) is shown in Fig. 4. It can be observed from the figure that convergence was a little erratic at first, indicating the value of the mid-cell back substitution procedure in helping to avoid divergence of the solution in the early stages of computation.

4 CONCLUSIONS

The procedure is particularly useful in the early stages of computation, where early detection of spurious solutions can avoid unnecessary computing time. The simulation of fluid flow in passages $< 20 \mu\text{m}$ in depth demonstrated a good deal of sensitivity to inlet boundary conditions, in addition to aspect ratios. The mid-cell back substitution technique avoided unnecessary pursuance of non-physical solutions.

The adoption of the mid-cell back substitution procedure can be used as an alternative to the 'staggered grid' technique [7], whereby the velocity and pressure components are calculated at separate grid locations. The staggered grid technique requires additional computer storage space, which is not necessary with the mid-cell back substitution procedure.

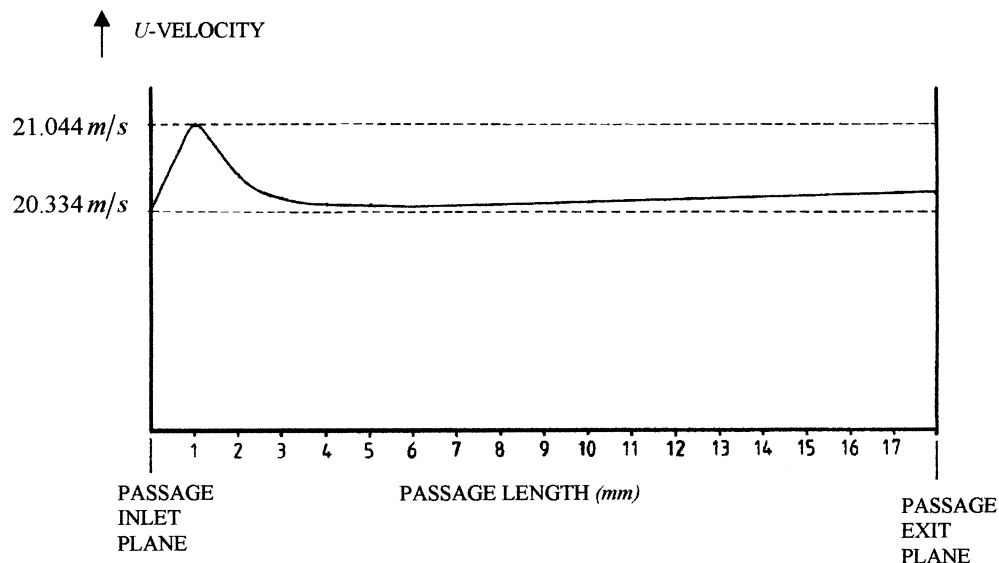
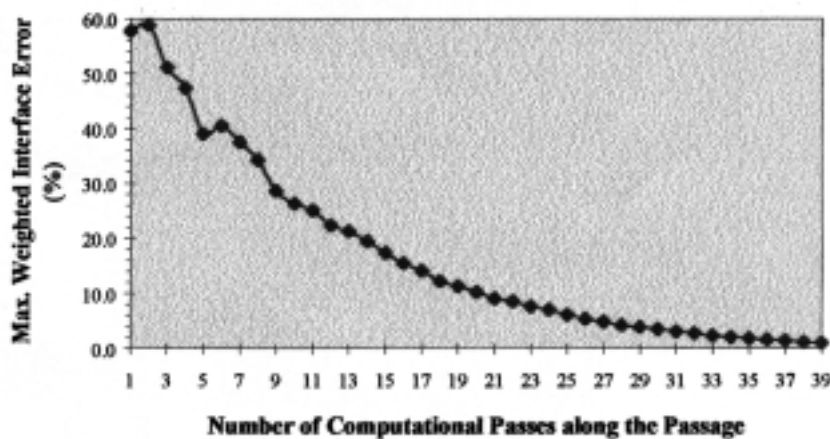


Fig. 3 Variation in the centre-line velocity u along the length of the passage

Table 1 Comparison between theoretical, computational and experimentally found friction factors in micron-sized passages

Passage depth and type of fluid respectively	Reynolds number Re	Friction factor f calculated using equation $f = 24/Re$	Friction factor f calculated from computational pressure variations along micropassages	Friction factor f calculated from experimental pressure variations along micropassages
30 μm , distilled water	13.2	1.818	2.349	2.463
30 μm , nitrogen gas	49.3	0.487	0.643	0.706
55 μm , distilled water	82.4	0.291	0.379	0.405
55 μm , nitrogen gas	109.6	0.219	0.239	0.239*
1 mm, distilled water	800	0.03	0.046	—

*Probable error ± 0.0207 **Fig. 4** Convergence of the computational procedure

REFERENCES

- Kendall, S. R.** Analysis of fluid flow through micron sized rectangular passages. PhD thesis, Chapter 4, Section 4.7 entitled 'Solution convergence', The University of Huddersfield, 1996.
- Raghavan, M. and Roth, B.** Solving polynomial systems for the kinetic analysis and synthesis of mechanism and robot manipulators. *Trans. ASME*, June 1995, **117**, 71–79.
- Stroud, K. A.** *Further Engineering Mathematics*, 1987, pp. 259–261 (Macmillan Education Limited).
- Press, W. H., Flannery, B. P., Teukolsky, S. A. and Vetterling, W. T.** *Numerical Recipes*, 1990, pp. 31–38 (Cambridge University Press).
- McAdams, W. H.** *Heat Transmission* 1958, pp. 155–159 (McGraw-Hill Book Company).
- Sucec, J.** *Heat Transfer*, 1985, pp. 434–435 (Wm C. Brown Publishers).
- Patankar, S. V.** *Numerical Heat Transfer and Fluid Flow*, 1980, pp. 115–126. (Hemisphere Publishing Corporation).

APPENDIX

If y_{i0} , $i = 1, 2, \dots, N$ are possible solutions to the N equations in (1), then the y_{i0} solution values can be denoted as follows:

$$y_{1,0}, y_{2,0}, \dots, y_{N_1,0} \equiv r_1, r_2, \dots, r_{N_1}$$

$$y_{N_1+1,0}, y_{N_1+2,0}, \dots, y_{N_1+N_2,0} \equiv s_1, s_2, \dots, s_{N_2}$$

$$y_{N_1+N_2+1,0}, y_{N_1+N_2+2,0}, \dots, y_{N,0} \equiv t_1, t_2, \dots, t_{N_3}$$

(14)

Thus, $r_1, r_2, \dots, r_{N_1}, s_1, s_2, \dots, s_{N_2}$, and t_1, t_2, \dots, t_{N_3} are the alternative nomenclature for the y_{i0} , $i = 1, 2, \dots, N$ values.

Also, let the equations in (1) be represented as follows:

- N_1 linear equations l_1, l_2, \dots, l_{N_1}
- N_2 quadratic equations q_1, q_2, \dots, q_{N_2}
- N_3 cubic equations c_1, c_2, \dots, c_{N_3}

Step A. Assume that $r_1, r_2, \dots, r_{N_1}, t_1, t_2, \dots, t_{N_3}$ and s_2, s_3, \dots, s_{N_2} are known. Substituting these values into the quadratic equation q_1 gives

$$F(s_1) = 0 \quad (15)$$

where $F(s_1)$ will be a quadratic expression of s_1 . Hence, in principle, two roots of s_1 are obtained from (3), which are represented as s_1^1 and s_1^2 .

Now, substituting $(r_1, r_2, \dots, r_{N_1}, t_1, t_2, \dots, t_{N_3}, s_1^1, s_3, \dots, s_{N_2})$ and $(r_1, r_2, \dots, r_{N_1}, t_1, t_2, \dots, t_{N_3}, s_1^2, s_3, \dots, s_{N_2})$ into the quadratic equation q_2 gives

$$F^1(s_2) = 0 \quad (16)$$

$$F^2(s_2) = 0 \quad (17)$$

where F^1 and F^2 are quadratic expressions of s_2 .

Hence, in principle, it is possible to find roots of s_2 as $s_2^1, s_2^2, s_2^3, s_2^4$. Thus, there are four possible sets of roots:

$$r_i, s_1^1, s_2^1, \dots, s_{N_2}, t_i$$

$$r_i, s_1^1, s_2^2, \dots, s_{N_2}, t_i$$

$$r_i, s_1^2, s_2^3, \dots, s_{N_2}, t_i$$

$$r_i, s_1^2, s_2^4, \dots, s_{N_2}, t_i$$

It is possible to proceed in this manner until 2^{N_2} sets of roots are obtained.

Step B. Consider that $r_1, r_2, \dots, r_{N_1}, s_1, s_2, \dots, s_{N_2}$ and t_2, \dots, t_{N_3} are known values. Then, substituting these values into equation c_1 will give

$$G(t_1) = 0 \quad (18)$$

where $G(t_1)$ is a cubic expression of t_1 .

In principle, there are three possible roots from t_1 , denoted as t_1^1, t_1^2 and t_1^3 . Now, substituting $r_1, r_2, \dots, r_{N_1}, s_1, s_2, \dots, s_{N_2}, t_1^1, t_3, \dots, t_{N_3}; r_1, r_2, \dots, r_{N_1}, s_1, s_2, \dots, s_{N_2}, t_1^2, t_3, \dots, t_{N_3};$ and $r_1, r_2, \dots, r_{N_1}, s_1, s_2, \dots, s_{N_2}, t_1^3, t_3, \dots, t_{N_3}$ into the cubic expression c_2 gives

$$G^1(t_2) = 0$$

$$G^2(t_2) = 0$$

$$G^3(t_2) = 0$$

(19)

where G^1, G^2, G^3 are cubic expressions of t_2 .

In principle, nine roots of t_2 can then be obtained. Let these roots be denoted by $t_2^1, t_2^2, t_2^3, \dots, t_2^9$. Hence, there are nine possible sets of roots and, continuing along these lines, 3^{N_3} possible sets of roots are obtained.

Step C. Since step A can be carried out with each of the possible 3^{N_3} sets of roots, t_1, t_2, \dots, t_{N_3} , a total of $(2^{N_2} \times 3^{N_3})$ sets of roots can be established.

Step D. For all the $(2^{N_2} \times 3^{N_3})$ sets of roots in step C, s_1, s_2, \dots, s_{N_2} and t_1, t_2, \dots, t_{N_3} , linear equations l_1, l_2, \dots, l_{N_1} can be set up for r_1, r_2, \dots, r_{N_1} . Hence, unique values are obtained for r_1, r_2, \dots, r_{N_1} for each of the sets of s_1, s_2, \dots, s_{N_2} and t_1, t_2, \dots, t_{N_3} .

Thus, the total possible sets of $r_1, r_2, \dots, r_{N_1}, s_1, s_2, \dots, s_{N_2}$ and t_1, t_2, \dots, t_{N_3} are given by

$$N_{\text{set}} = 2^{N_2} \times 3^{N_3} \quad \text{for } i = 1, 2, \dots, N \quad (1)$$